Conformational Change Rate-Limits GTP Hydrolysis: The Mechanism of the ATP Sulfurylase−GTPase†

Jiang Wei and Thomas S. Leyh*

Department of Biochemistry, Albert Einstein College of Medicine, 1300 Morris Park Avenue, Bronx, New York 10461

Received July 20, 1998; Revised Manuscript Received September 25, 1998

ABSTRACT: The fluorescent GTP analogues 3′-*O*-(*N*-methylanthraniloyl)-2′-deoxyguanosine 5′-(β,γ-imidotriphosphate) (mGMPPNP) and 3′-*O*-(*N*-methylanthraniloyl)-2′-deoxy-GTP (mGTP) were used to demonstrate that an enzyme isomerization precedes and rate-limits β,γ-bond cleavage in the catalytic cycle of the ATP sulfurylase−GTPase, from *E. coli K-12*. The binding of mGMPPNP to the E·AMP·PP_i complex of ATP sulfurylase is biphasic, indicating that an isomerization occurs in the binding reaction. The isomerization mechanism was assigned based on the results of the enzyme concentration dependence of the observed rate constants, k_{obs}, for both phases of the binding reaction, and sequential-mixing, nucleotide release experiments. The isomerization occurs after, and is driven by, the addition of mGMPPNP. Values were determined for each of the rate constants associated with the two-step kinetic model used in the interpretation of the results. A comparison of the enzyme concentration dependence of k_{obs} for the hydrolysis and binding reactions reveals that the rate constants for the corresponding steps of these two reactions are extremely similar. The virtually identical rate constants for isomerization and β,γ-bond scission strongly suggest that isomerization rate-limits bond breaking. The implications of these finding for GTPase/target interactions and the mechanism of energetic linkage in the ATP sulfurylase system are discussed.

GTPases are widely used to transfer information within the communication network of the cell. These signaling proteins transmit the information that a particular event has occurred at some point(s) in the cell, to a target or recipient, which may reside elsewhere (*1*). The imprinting of this molecular information is achieved through conformational changes in the GTPase that are catalyzed during its interactions with the donor and recipient (*2*). The donor interactions produce a GTPase·GTP complex that is prepared to recognize its target. The activities of the GTPase and target are controlled by allosteric interactions that occur in the GTPase·target complex. Activation of the target typically ceases upon hydrolysis of GTP; hence, the lifetime of GTP in the complex determines the duration of the target's activation (*3*).

The question of whether a conformational change precedes and rate-limits GTP hydrolysis is central to the nature of the interactions that occur in the GTPase·target complex: is protein isomerization or hydrolysis, per se, manipulated by these interactions? This question has been addressed in two other GTPase systems. The Ef-Tu literature supports a rate-limiting conformational change (*4*); however, the RAS literature remains equivocal on this point (*5*−*8*). In this paper, we investigate this issue with the ATP sulfurylase−GTPase system using the fluorescent, 3′-*O*-(*N*-methylanthraniloyl) derivatives of 2′-deoxy-GTP and -GMPPNP (*9, 10*). Our results strongly support that the ATP sulfurylase−GTPase undergoes an isomerization, after the binding of nucleotide, that precedes and rate-limits the hydrolysis of GTP.

† Supported by National Institutes of Health Grant GM 54469.

* Address correspondence to this author at the Department of Biochemistry, Albert Einstein College of Medicine, 1300 Morris Park Ave., Bronx, NY 10461. Telephone: 718-430-2857. Fax: 718-430-8565. E-mail: Leyh@aecom.yu.edu.

ATP sulfurylase (ATP:sulfate adenylyltransferase, EC 2.7.7.4), from *E. coli K-12*, catalyzes and couples the chemical potentials of GTP hydrolysis and the synthesis of activated sulfate (adenosine 5′-phosphosulfate, or APS), reactions 1 and 2 (*11, 12*):

$$GTP + H_2O \rightleftharpoons GDP + P_i + H^+ \quad (1)$$

$$ATP + SO_4 \rightleftharpoons APS + PP_i \quad (2)$$

The native enzyme is a tetramer of heterodimers (*13*); each dimer is composed of a GTPase, CysN (53 kDa), and its target, CysD (35 kDa) (*14*). Activated sulfate is an essential intermediate in the biosynthesis of reduced sulfur metabolites in aerobic bacteria (*15*). In anaerobes, the reduction of APS serves as a primary electron sink to thermodynamically draw electrons through the transport chains that drive oxidative phosphorylation (*16*). Mammalian systems use activated sulfate as a sulfuryl-group donor. Sulfuryl transfer, much like phosphoryl transfer, regulates the metabolic activity of the recipient (*17, 18*). How the free energies of GTP hydrolysis and APS synthesis are coupled by the catalytic cycle of ATP sulfurylase is a fundamental question in this system. The isomerization that controls GTP hydrolysis appears to be driven by the formation of an enzyme intermediate that occurs during APS synthesis. This interdependence of the GTP hydrolysis and APS-forming reactions is an important aspect of the linking mechanism.

MATERIALS AND METHODS

Materials. Guanosine 5′-(β,γ-imidotriphosphate) (GMPPNP), AMP (free acid), ampicillin, 2′-deoxyguanine nucle-

10.1021/bi9817461 CCC: $15.00
Published on Web 11/18/1998

otides (sodium salt), Hepes,[1] imidodiphosphate (PNP), lysozyme, $MgCl_2$, Na_4EDTA,[1] streptomycin sulfate, and Tris[1] were purchased from the Sigma Chemical Co. 1,1′-Carbonyldiimidazole, tributylamine (TBA), hexamethylphosphoric triamide (HMP), triethylamine (TEA), and chloroform were purchased from the Aldrich Co. *N*-Methylisatoic anhydride was obtained from Molecular Probes, Inc. All of the enzymes used in the construction of the ATP sulfurylase expression plasmid, pTL9, were from New England Biolabs and Boehringer Mannheim. Isopropylthio-β-galactoside (IPTG) was from Gibco BRL. Oligonucleotides were from the Einstein DNA synthesis facility. BL21(DE3) and pET-23a were from Stratagene.

The ATP Sulfurylase Expression System. The previous ATP sulfurylase expression plasmid, pTL1, contained the *cysDNC* promoter immediately upstream of the ATP sulfurylase coding regions, *cysDN*. Maximum expression of ATP sulfurylase requires that the *cysDNC* promoter be derepressed by growing cells containing pTL1 in minimal media with sulfate as a sole sulfur source. To allow expression in rich media, the *cysDN* coding region was excised from pTL1 and inserted into the T7-based expression vector, pET-23a. Excision was accomplished using an oligonucleotide-directed, PCR-based strategy. The insert of the resulting expression plasmid, pTL9, was ligated, at its 5′-terminus, to pET-23a at the *Nde*I site that contained the *cysD* initiation codon. At its 3′ terminus, the insert was blunt-end-ligated into the vector using the insert's *Sna*BI site, located 161 base pairs 3′ of the adenine in the *CysC* start codon, and the *Hin*cII site of the vector. Both strands of the insert were sequenced at the Einstein sequencing facility; the insert sequence exactly matched that of the published sequence (*14*).

The *E. coli* strain BL21(DE3) was transformed with pTL9 using standard methods (*19*). The transformed cells were grown at 37 °C to an $OD_{600} = 0.6$, IPTG was added to 0.40 mM, and the cells were incubated at 37 °C for 2 h and harvested. The purification of the enzyme yielded ∼100 mg of ATP sulfurylase per liter of culture.

ATP Sulfurylase. The enzyme was purified according to a published protocol (*13*) from the BL21(DE3)/pTL9 strain described in the preceding two paragraphs. The specific activity of the pure enzyme was 0.64 unit/mg (*13*).

The Synthesis of 3′-O-(N-Methylanthraniloyl)-2′-deoxyguanosine 5′-(β,γ-Imidotriphosphate) (mGMPPNP) and 3′-O-(N-Methylanthraniloyl)-2′-deoxy-GTP (mGTP). 2′-Deoxy-GMPPNP was synthesized according to a previously published protocol (*20*). Briefly, 1.0 mmol of the TBA salt of 2′-deoxy-GMP, in 2.0 mL of HMP, was mixed with 1.6 mmol of 1,1′-carbonyldiimidazole in 5.0 mL of HMP. The mixture was stirred for 30 min and placed over P_2O_5 in an evacuated desiccator for 5 h. A mixture of 0.50 mL (12 mmol) of anhydrous MeOH and 1.0 mL of HMP was then added to the reaction. Five hours later, 5.0 mmol of PNP (TBA salt), in 10 mL of HMP, was added with vigorous mixing, and the reaction was allowed to stand for 12 h. The nucleotide was extracted with 125 mL of a solution containing 100 mL of chloroform, and 25 mL of water. The aqueous phase, which contained the 2′-deoxy-GMPPNP, was dried by rotary evaporation, suspended in 20 mL of water, and the pH was adjusted to 8.0 using 3.0 N KOH.

The 2′-deoxy-GMPPNP was purified in three chromatographic steps. The first used a 2.5 × 8.0 cm bed of DEAE Sepharose and a 600 mL, 0.050−1.0 M, linear gradient of TEA/HCO_3^-; 2′-deoxy-GMPPNP eluted at 0.50 M. The second used a Mono Q 10/10 column, FPLC gradient system, with a 0.2−1.0 M linear gradient of TEA/HCO_3^-; 2′-deoxy-GMPPNP eluted at 0.70 M. The 2′-deoxy-GMPPNP was purified to >95% by reverse-phase chromatography using a Waters, μBondpak, C-18 column, with an isocratic running buffer [96% 10 mM phosphate (sodium salt), pH 6.0: 4% acetonitrile].

The structure of the 2′-deoxy-GMPPNP was confirmed by ^1H and ^{32}P nuclear magnetic resonance (NMR). One-dimensional ^1H spectra of 2′-deoxy-GMPPNP (1 mM) in 90% D_2O were recorded, at 25 ± 2 °C, with a Bruker AMX 500 spectrometer. The delay and acquisition times were both 3.0 s. The chemical shifts and coupling constants of the ^1H spectrum closely matched those of a control spectrum of 2′-deoxy-GMP. One-dimensional ^{32}P spectra of 2′-deoxy-GMPPNP (1.0 mM) in 90% D_2O were recorded, at 25 ± 2 °C, with a Bruker DRX 300 spectrometer. The spectrum of the compound at pH 9.2, $[MgCl_2] = 2.0$ mM, displayed the splitting pattern diagnostic for the $\beta-\gamma$ imido linkage (*21*), and closely matched that of a control spectrum of GMPPNP obtained under the same conditions. The delay and acquisition times were 2.0 and 3.0 s, respectively.

The 3′-*O*-(*N*-methylanthraniloyl) derivatives of 2′-deoxy-GTP and 2′-deoxy-GMPPNP were prepared as previously described (*10*, *22*, *23*). The purity of these compounds was assessed at >95% based on 252 nm chromatographic profiles obtained using C-18 HPLC.

Stopped-Flow Fluorescence Measurements. Measurements were made using a Photophysics (Model SX-17MV) instrument. The samples were equilibrated and experiments performed at 25 ± 2 °C. The excitation wavelength was 350 nm; light emitted above 400 nm was detected. A typical experiment used a 300 V photomultiplier gain with variable bias offset. The signals were acquired without filtering; five to seven scans were averaged. The data were fit and the experimental uncertainties were obtained using the Photophysics data analysis software which employs a Marquardt fitting algorithm. The sequential-mixing experiments were performed using the same model instrument with an SQ1 sequential-mixing accessory. A 700 V photomultiplier gain was used with a variable bias offset. The concentration dependence of reaction rates was evaluated by varying the enzyme, rather than ligand, concentration. This strategy, in which the concentration of the nonfluorescent species is varied, considerably improves the quality of the data and simplifies performing these experiments by allowing all of the data to be collected at a single instrumental setting. Varying the mant-nucleotide, which is intensely fluorescent, requires regular resetting, and therefore recalibration of the instrument, due to saturation of the detector.

Quench-Flow Experiments. The experiments were performed with a KinTek quench-flow apparatus. A solution containing ATP sulfurylase (40 μM), AMP (1.0 mM), $MgCl_2$ (2.1 mM), PP_i (100 μM), and Hepes (50 mM, $pH/K^+ = 8.0$) was rapidly mixed with a solution that was identical except

[1] Abbreviations: EDTA, ethylenediamine-*N*,*N*,*N*′,*N*′-tetraacetic acid; Hepes, 4-(2-hydroxyethyl)-1-piperazineethanesulfonic acid; Tris, tris-(hydroxymethyl)aminomethane; unit, micromoles of substrate converted to product per minute at V_{max}.

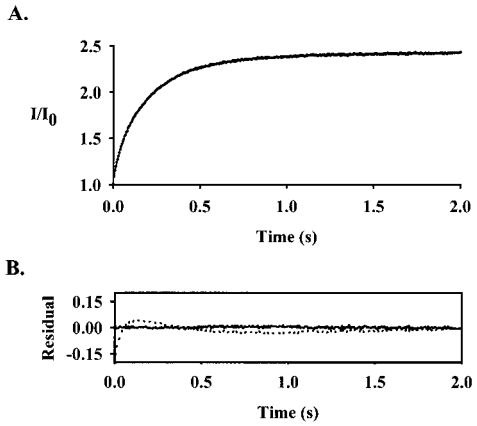

FIGURE 1: Binding of mGMPPNP to the E·AMP·PP_i complex of ATP sulfurylase. Panel A: The progress curve for the binding reaction. The progress of the reaction was monitored by following the change in fluorescent intensity of mGMPPNP as it interacts with the enzyme (see Materials and Methods). The reaction was initiated by mixing a solution containing ATP sulfurylase (40 μM), AMP (1.0 mM), $MgCl_2$ (2.1 mM), PP_i (100 μM), and Hepes (50 mM, pH/K^+ = 8.0) with an equal volume of an identical solution that did not contain enzyme, but did contain mGMPPNP (4.0 μM). The solutions were preequilibrated, and the experiments were performed, at 25 (±2) °C. The smooth curve passing through the data represents the best fit to a double-exponential model. Panel B: The residual plots obtained using single exponential (dotted line) and double exponential (solid line) models to fit the data.

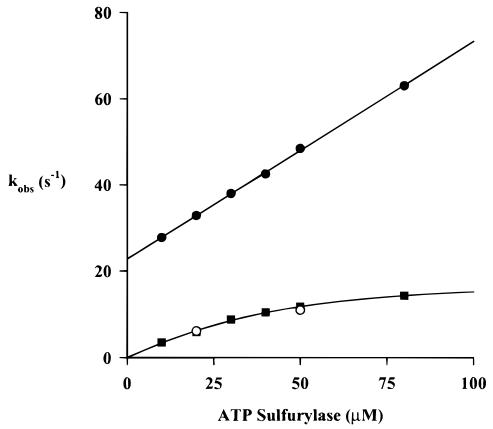

FIGURE 2: Enzyme concentration dependence of the observed rate constants for the first ($k_{1(obs)}$) and second ($k_{2(obs)}$) phases of the mGMPPNP binding reaction. The experimental conditions were identical to those described in the Figure 1 legend except that the ATP sulfurylase concentration was varied as indicated. The closed circles (●) and squares (■) represent $k_{1(obs)}$ and $k_{2(obs)}$, respectively. The open circles (○) represent the values obtained from mGTP hydrolysis experiments performed under the same conditions (see *Conformational Change Rate-Limits Hydrolysis*).

that it did not contain enzyme, but did contain mGTP (400 μM). The reactions were allowed to proceed for a given time interval before quenching by rapid mixing with an equal volume of 100 mM Na_4EDTA (pH 9.5). The samples were equilibrated, and the experiments were performed at 25 ± 2 °C. The mGTP and mGDP were separated using a Waters, μBondpak, C-18 column, with an isocratic running buffer [96% 10 mM phosphate (sodium salt), pH 6.0: 4% acetonitrile]. mGTP and mGDP were detected using a fluorescence detector, and quantitated by referencing their peak areas to standard curves constructed using the same nucleotides.

RESULTS AND DISCUSSION

Isomerization in the Binding Reaction. The nonhydrolyzable, fluorescent analogue of GTP, mGMPPNP, was used in stopped-flow fluorescence experiments to investigate whether an isomerization occurs in the nucleotide binding reaction. This analogue accurately mimics the interactions of GTP with ATP sulfurylase and other GTPases (*9, 22, 24*−*26*). To avoid the complications associated with 2′-3′ transesterification of the fluorophore, which changes its fluorescent properties, our studies used the 2′-deoxy analogues exclusively (*6, 9*). The E·AMP·PP_i complex of ATP sulfurylase was used in the binding reactions. The GTP hydrolysis k_{cat} associated with this complex is 120-fold greater than that for the unliganded form of the enzyme (*27*). These activators are believed to elicit a form of the enzyme that resembles the E·*AMP·PP_i intermediate that occurs in the GTP-coupled, APS synthesis reaction (*27*).

The progress curve for the binding reaction is presented in panel A of Figure 1. The residual plot obtained when the data are fit using a single-exponential model demonstrates that nucleotide binding is not well represented by a first-order process (dotted line, panel B, Figure 1). The residual plot obtained using a double-exponential model indicates that the binding reaction is at least biphasic and that it is well described by a two-step mechanism (solid line, panel B, Figure 1). Thus, it appears that the mechanism includes an isomerization step.

To confirm that an isomerization occurs, and to obtain values for certain of the rate constants in the two-step model, the enzyme concentration dependence of the observed rate constants for the first and second phases, $k_{1(obs)}$ and $k_{2(obs)}$, of the binding reaction were determined. The experimental conditions of this study were similar to those for the progress curve described above. All of the reactions were pseudo-first-order with respect to enzyme concentration. The results, presented in Figure 2, demonstrate that $k_{1(obs)}$ is linearly dependent on enzyme concentration, and that the $k_{2(obs)}$ dependence is hyperbolic. This is the expected result for a two-step isomerization mechanism in which ligand adds to only one of the enzyme isomers, and the isomerization is slow compared to the addition of ligand (*28*). These results do not determine whether isomerization occurs before, or after, the addition of ligand. In either case, isomerization is thermodynamically driven by the addition of ligand. The quantitation of the model is described below (see *Quantitating the Model*).

The Isomerization Mechanism. Whether isomerization precedes, or is subsequent to the addition of ligand can be determined by evaluating the kinetics of ligand release from the enzyme. If the enzyme isomerizes prior to ligand addition, a single enzyme·ligand complex is formed, and release, occurring in a single step, will be monophasic. If isomerization occurs after binding, two steps are required to complete the release, which, in general, predicts a biphasic progress curve; however, detecting both phases requires a favorable set of rate constants and amplitudes. For example, if the equilibrium constant for the isomerization is too far in either direction, the signal from one of the complexes will not be detected; or, if the isomerization step is at equilibrium during release, monophasic behavior is observed.

The number of phases in the release reaction can be determined by monitoring the progress of a reaction initiated

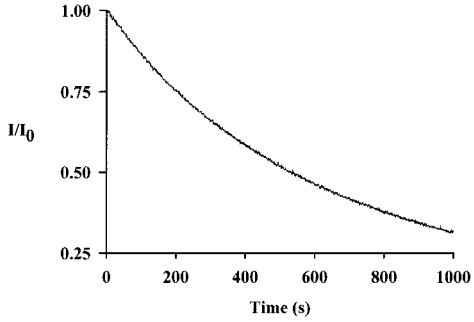

FIGURE 3: Irreversible dissociation of mGMPPNP from the mGMPPNP·E·AMP·PP_i complex. The release of mGMPPNP was monitored in a stopped-flow fluorescence experiment in which mGMPPNP was displaced from ATP sulfurylase using GMPPNP. A solution containing ATP sulfurylase (40 μM), mGMPPNP (4.0 μM), AMP (1.0 mM), $MgCl_2$ (2.1 mM), PP_i (100 μM), and Hepes (50 mM, pH/K^+ = 8.0) was mixed with an equal volume of an identical solution that did not contain enzyme and mGMPPNP but did contain GMPPNP at 400 μM, a concentration sufficient to displace >98% of the mGMPPNP from the enzyme. The solutions were preequilibrated, and the experiments were performed, at 25 (±2) °C.

by rapidly mixing an equilibrated solution of enzyme and fluorescent ligand (i.e., mGMPPNP) with a nonfluorescent, competitive ligand (i.e., GMPPNP). The analysis of the result is simplified if the concentration of the nonfluorescent ligand is sufficient to ensure that the release of the fluorophore is essentially irreversible.

The result of such an experiment is shown in Figure 3. In this experiment, an equilibrated solution of ATP sulfurylase, mGMPPNP, AMP, and PP_i was rapidly mixed with a solution that was identical except that it did not contain enzyme and mGMPPNP, but did contain GMPPNP at a concentration sufficient to drive 98% of the mGMPPNP into solution (0.20 or 2.0 mM); k_{obs}, 0.0017 ± 0.0001 s^{-1}, was independent of the GMPPNP concentration. Thus, while this experiment provided k_{obs} for the release, which will prove useful later, it was inconclusive on the issue of mechanism.

To investigate further the isomerization mechanism, a sequential-mixing experiment was performed that allowed the detection of intermediates that accumulate during the binding reaction, but are undetectably low at equilibrium. The experiment is conceptually similar to that described in the preceding paragraph. The binding reaction is initiated by mixing a solution containing E with one containing the fluorescent ligand L. The reaction is allowed to proceed for a defined time interval, the delay time, at the end of which it is mixed with a solution containing a nonfluorescent, competitive ligand. Dual mixing allows control over the point in the binding reaction at which the irreversible release of the fluorophore is initiated. If the binding and dissociation of ligand and E are fast compared to E′·L formation, E·L will accumulate in the early stage of the binding reaction. If release is initiated during this early stage, E·L will dissociate quickly compared to E′·L, and a biphasic release will be observed. The amplitude of the first phase will increase to a maximum as E·L forms, and then decay as it is converted to E′·L. The amplitude of the second phase will increase with delay time as the concentration of E′·L increases, and plateau as the reaction achieves equilibrium.

The results of a series of two-stage mixing experiments in which the delay time was varied are displayed in Figure

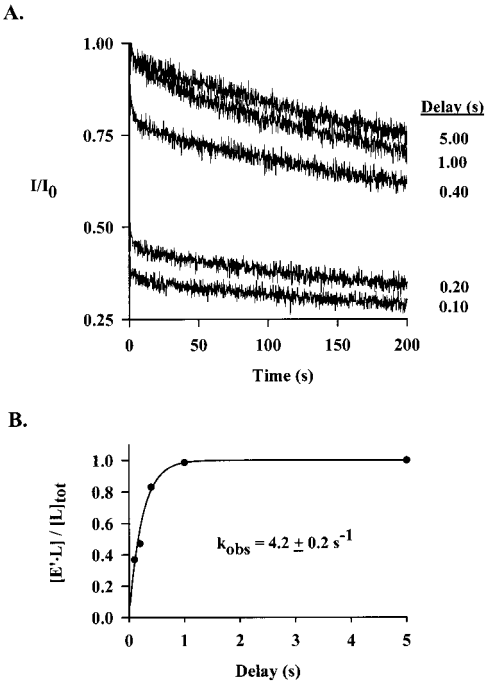

FIGURE 4: Initiating irreversible dissociation of mGMPPNP from the mGMPPNP·E·AMP·PP_i complex at sequential points in the binding reaction. Panel A: The progress curves for the dissociation reactions. The first mix of this two-stage mixing experiment initiates the binding reaction—the conditions were identical to those associated with Figure 1. At the end of a variable delay period that follows the first mix, the reacting solution is mixed with a equal volume of an identical solution that did not contain enzyme or mGMPPNP, but did contain GMPPNP (400 μM). The second mix initiates the dissociation of mGMPPNP. The progress curves are clearly biphasic. Panel B: Formation of the E′·L complex vs delay time. The second phase amplitude at each delay time was obtained by fitting the 5−200 s interval for each curve to a single-exponential function. The resulting amplitudes were divided by the amplitude associated with the 5 s delay interval to obtain the values of [E′·L]/$[L]_{tot}$. At the 5 s interval, virtually all of the ligand resides in the E′·L complex. The plot of [E′·L]/$[L]_{tot}$ vs delay time was well fit by a single-exponential function (solid line) with a k_{obs} = 4.2 s^{-1}.

4. In each experiment, the binding reaction was initiated by mixing a solution containing ATP sulfurylase, AMP, $MgCl_2$, and PP_i with a concentration-matched solution that did not contain enzyme, but did contain mGMPPNP. The reaction progressed during the delay period, at the end of which it was mixed with a matched solution without enzyme, and containing GMPPNP (400 μM). The desorption reaction was monitored following the second mix. As is shown in panel A of Figure 4, the progress curves at various delay intervals are biphasic, except at the longest delay time, at which point the reaction is near equilibrium. The first phase of each biphasic curve is essentially complete within the first few data points, and the amplitude of this phase decreases with increasing delay time. The second phase is relatively slow, and its amplitude increases with increasing delay time. The biphasic nature of these curves clearly demonstrates that the binding mechanism is one in which isomerization occurs after the addition of ligand.

Plotting the amplitude of the second phase vs delay time provides a progress curve for the accumulation of the species that forms during the second phase (i.e., E′·L). This plot, shown in panel B of Figure 4, is monophasic with a k_{obs} of 4.2 ± 0.2 s^{-1}. This value is identical to k_{obs} for the second

$$E + L \underset{7.9\ s^{-1}}{\overset{2.9 \times 10^5\ M^{-1}\ s^{-1}}{\rightleftharpoons}} E{\cdot}L \underset{0.0047\ s^{-1}}{\overset{14\ s^{-1}}{\rightleftharpoons}} E'{\cdot}L$$

FIGURE 5: Two-step model for the binding of mGMPPNP to the E·AMP·PP_i complex of ATP sulfurylase. The rate constants were calculated from data presented in the text (see *Quantitating the Model*). The equilibrium constant associated with the second step is 2980, which corresponds to a $\Delta G^{\circ\prime}$ of −4.7 kcal/mol at pH 8.0 and 25 °C.

phase of the binding reaction shown in Figure 1. The conditions of the binding reactions associated with Figures 1 and 5 were identical. Thus, the similarity of these rate constants provides compelling confirmation of an isomerization step in the binding reaction.

Quantitating the Model. The four kinetic constants associated with the two-step isomerization model were obtained by statistically fitting the data shown in Figures 2 and 3. The k_{obs} vs enzyme concentration for the fast phase and slow phases of the GMPPNP binding reaction (Figure 2) are well described by eqs 3 and 4, in which k_1, k_{-1} and k_2, k_{-2} are the forward and reverse rate constants for the first and second steps, respectively, of the two-step model (*28*, *29*):

$$k_{1(obs)} = k_1[E] + k_{-1} + k_2 + k_{-2} \quad (3)$$

$$k_{2(obs)} = (k_1[E](k_2 + k_{-2}) + k_{-1}k_{-2})/(k_1[E] + k_{-1} + k_2 + k_{-2}) \quad (4)$$

Equation 3 is that of straight line with slope k_1 and intercept ($k_{-1} + k_2 + k_{-2}$). Equation 4 has the form of a rectangular hyperbola which, in the plateau, is equal to $k_2 + k_{-2}$. The best-fit values for the slope, intercept, and plateau are 2.9 (±0.1) M^{-1} s^{-1}, 22 (±0.2) s^{-1}, and 14 (±0.9) s^{-1}, respectively. Subtracting the plateau from the intercept provides k_{-1} [i.e., 7.9 (±0.9) s^{-1}]. The result obtained from the single-mix release experiment (Figure 3) was used to sort out k_2 and k_{-2}. The k_{obs} obtained from fitting these data, 0.0017 (± 0.0001) s^{-1}, is given by eq 5 (*30*):

$$k_{obs} = k_{-2}[k_{-1}/(k_{-1} + k_2 + k_{-2})] \quad (5)$$

The quotient in the brackets of eq 5 is calculated at 7.9/22. Thus, one can calculate that k_{-2} = 0.0047 (±0.0006) s^{-1} and k_2 = 14 (±0.9) s^{-1}. The isomerization mechanism and its associated rate constants are shown in Figure 5. From these rate constants, one can calculate that the equilibrium constant for the formation of E′·L from E·L, K_{iso}, is 2980. Thus, the internal, or enzyme-bound isomerization equilibrium constant corresponds to a standard Gibbs potential of −4.7 kcal/mol.

Conformational Change Rate-Limits GTP Hydrolysis. Whether isomerization is the rate-limiting step in the catalytic cycle is fundamental to the mechanism of GTPase/target interactions. The generally accepted model for these interactions is one in which the binding of GTPase·GTP complex and its target results in interactions that stabilize events associated with bond cleavage and thereby increase the rate of GTP hydrolysis (*1*−*3*, *31*). This model assumes that bond breaking is the slowest step in the catalytic cycle—if this were not true, the stabilization would not affect k_{cat} significantly. Alternatively, if isomerization is rate-limiting, then the allosteric interactions that regulate hydrolysis must focus upstream in the reaction coordinate from the cleavage step(s) to the region where the events that control the conformational change occur. In general, bond breaking appears to be concomitant with a switching of the kinetic parameters of the target from the active to inactive state; hence, controlling the isomerization also controls the catalytic disposition of the target.

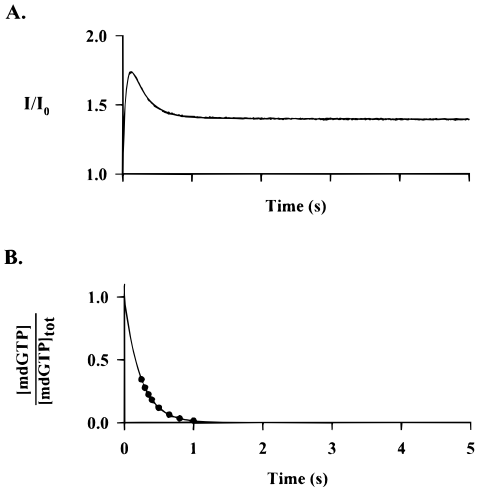

FIGURE 6: Hydrolysis of mGTP by the E·AMP·PP_i complex of ATP sulfurylase. Panel A: The stopped-flow fluorescence experiment. The progress of the reaction was monitored by following the change in fluorescent intensity of mGTP as it binds to, and is hydrolyzed by the enzyme. The conditions were identical to those described in Figure 1 except that mGMPPNP was replaced by mGTP. The solid line through the data is the outcome predicted by the best-fit two-step model. The observed rate constants for the two phases [$k_{1(obs)}$ = 21 (±1) s^{-1} and $k_{2(obs)}$ = 4.4 (±0.1) s^{-1}] are, within experimental error, equal to those associated with the progress curve shown in Figure 1. Panel B: The quench flow experiment. The conditions of the experiment were identical to those described in panel A. The reactions were allowed to progress for the indicated time interval before mixing with an equal volume of a quench solution containing 100 mM EDTA (pH 9.5). mGDP and mGTP were separated and quantitated as described under Materials and Methods. The observed rate constant for the hydrolysis reaction, k_{hyd}, was 4.4 (±0.1) sec^{-1}.

To assess whether the isomerization rate-limits GTP hydrolysis in the ATP sulfurylase−GTPase catalytic cycle, the observed rate constant for the hydrolysis of mGTP, k_{hyd}, was determined and compared to that for the isomerization with mGMPPNP, k_{iso}, under identical conditions. If these constants are significantly different, isomerization is not rate-limiting and may or may not be tightly coupled to hydrolysis. Identical values for k_{hyd} and k_{iso} suggest that they are obligately linked to one another.

The different quantum yields associated with the AMP·PP_i·E·mGMPPNP and AMP·PP_i·E·mGDP complexes suggested that hydrolysis could be monitored by a change in fluorescence. The results of a stopped-flow fluorescence study designed to monitor mGTP hydrolysis are shown in panel A of Figure 6. The conditions of this experiment were identical, except for the nucleotide, to those used in the mGMPPNP binding studies associated with Figure 1. The progress curve is biphasic, $k_{1(obs)}$ = 21 (±1) s^{-1} and $k_{2(obs)}$ = 4.4 (±0.1) s^{-1}. These constants are, within experimental error, identical to those associated with the mGMPPNP binding and isomerization reactions.

Quenched-flow experiments were performed to confirm that k_{obs} for the hydrolysis reaction is equivalent to that for

the second phase of the stopped-flow experiment, $k_{obs(2)}$. In the quench experiment, reactants are rapidly mixed, aged for a defined period, and then quenched by rapid mixing with a equal volume of Na_4EDTA (100 mM, pH 9.5). The reactants are separated by HPLC and quantitated (see Materials and Methods). The reaction conditions were identical for the quenched- and stopped-flow experiments. The progress curve for the hydrolysis of mGTP obtained from the quench experiments is shown in panel B of Figure 6. The k_{hyd} obtained from a single-exponential fit of the quench data, 4.4 ($\pm$0.1) s^{-1}, is, within experimental error, equal to the $k_{obs(2)}$ from the mGTP experiment. Thus, the second phase of the mGTP progress curve reports on the rate of at which the β,γ-bond is cleaved.

The near-equivalence of the observed rate constants for hydrolysis and isomerization supports that the isomerization, which precedes hydrolysis, rate-limits the catalytic cycle. These similarities in the rates of isomerization and hydrolysis suggest, but do not prove, that the microscopic rate constants that govern them are also similar. Similar k_{obs} values, determined at a single enzyme concentration, can also be explained by two very different sets of microscopic rate constants that happen to yield similar values for k_{obs} at a particular enzyme concentration. This uncertainty is reduced considerably for a two-step mechanism if $k_{obs(1)}$ and $k_{obs(2)}$ for isomerization and hydrolysis show similar enzyme concentration dependencies. Stopped-flow experiments, performed under identical conditions, reveal that $k_{obs(1)}$ and $k_{obs(2)}$ are virtually identical for the mGMPPNP and mGTP reactions at two well-separated enzyme concentrations (see open and closed circles, Figure 2). Suitable manipulation of eqs 3 and 4 shows that for two separate two-step processes to have identical values for $k_{obs(1)}$ and $k_{obs(2)}$ at different enzyme concentrations, the following conditions must hold: $k_1 = k_1'$; $k_{-1} = k_{-1}'$; and $(k_2 + k_{-2}) = (k_2' + k_{-2}')$—the primed and nonprimed constants are associated with hydrolysis and isomerization, respectively. Thus, the question of the similarity of the rate constants reduces to sorting out the differences between k_2 and $k_{2'}$ and/or k_{-2} and $k_{-2'}$. This is easily accomplished if, as was shown above for the isomerization reaction, $k_2 \gg k_{-2}$; then, $(k_2 + k_{-2}) = (k_{2'} + k_{-2'}) \sim k_2$, and, therefore, $k_{2'} \leq k_2$. If $k_{2'}$, the rate constant for the bond breaking step, were significantly less than k_2, the rate constant for the forward isomerization step, hydrolysis would be at least partially rate-limiting and the observed rate constant for hydrolysis would be less than that for isomerization, which is not observed; therefore, $k_{2'} \sim k_2$ and $k_{-2'} \sim k_{-2}$.

The preceding discussion illustrates that, for a two-step model, the magnitudes of the rate constants for the corresponding steps of the hydrolysis and isomerization reactions are extremely similar. Thus, the activation energies for hydrolysis and isomerization are virtually identical, and isomerization, therefore, appears to control hydrolysis.

Other GTPases. The existence of a rate-limiting, prehydrolytic conformational change has been investigated using GTPases from several GTPase classes. The catalytic cycle of elongation factor Tu (EF-Tu), a GTPase that binds to, and delivers, amino-acylated tRNA to ribosomes engaged in polypeptide elongation, appears to include such an isomerization. Delivery of the charged amino acid to the elongating polypeptide first requires appropriate codon−anticodon recognition, and the hydrolysis of GTP. Recognition appears to drive an EF-Tu isomerization that enables it to hydrolyze GTP (*4*, *32*). Studies using G_o and G_α, two members of the heterotrimeric G-protein family, have identified a substrate-induced conformational change that is required for the interaction of the G-protein and its target; this isomerization has not yet been correlated with hydrolysis (*25*, *33*). This isomerization issue has been studied extensively using the proto-oncogene RAS, a member of the p21 GTPase family (*5*−*8*, *34*, *35*). Due to what appear to be methodological differences, the RAS studies have produced conflicting results; hence, the issue remains unresolved.

Nominally, two of the four systems studied (i.e., ATP sulfurylase and EF-Tu) demonstrate a rate-limiting isomerization in their catalytic cycles. In both cases, see the preceding and following paragraphs, allosteric manipulation of the isomerization regulates turnover. While it seems likely that such isomerizations occur in other GTPases, generalizations regarding the ubiquity of this mechanistic element within the superfamily must, at present, be tempered by the paucity of data on this topic.

Implications for the Coupling of GTP Hydrolysis and APS Synthesis. GTP hydrolysis immediately precedes, or is concomitant with, cleavage of the $\alpha-\beta$ bond of ATP (*36*). The steps that link these two bond-breaking events form the basis of the energetic coupling in this system. In the absence of activators, the rate of GTP hydrolysis is quite low, $k_{cat} = 0.01\ s^{-1}$ (*27*), and we do not observe a significant second phase upon binding of mGMPPNP (data not shown). At saturating concentrations of AMP and PP_i, the k_{cat} for GTP hydrolysis is stimulated 120-fold, and, as described above, a second phase is associated with the binding reaction (*27*). While it is possible that isomerization does not occur, or is not associated with a fluorescence change in the absence of activators, we prefer an interpretation that requires neither a fundamentally different mechanism nor a change in the properties of the intermediates, that is, that the activators drive the system into the isomerized form, from which hydrolysis occurs. Confirmation of this interpretation requires further experimentation; however, regardless of mechanism, it is clear that the binding of activators alters the GTPase active site, enabling it to accomplish catalysis at the activated rate. It is as if the catalytic machinery has been snapped into is active configuration by the activator-induced isomerization.

ATP sulfurylase conformationally couples the chemical potential of GTP hydrolysis to that of activated sulfate synthesis (*11*, *12*). Conformational coupling is achieved through allosterically driven structural changes that link events that occur in the separate reactions to one another. These structural signals gate the movement of each reaction between successive points in its reaction coordinate. The resultant interdependence fixes the stoichiometry of the reactions and couples their free energies (*11*, *37*, *38*). The AMP/PP_i-induced conformational change that stimulates hydrolysis demonstrates how ATP sulfurylase couples the two chemistries—the arrival of the APS reaction at the appropriate point in its catalytic cycle initiates an acceleration of the isomerization reaction and, hence, hydrolysis. While these findings reveal certain of the intricacies that control the linkage in this system, others remain enigmatic. We do not yet fully understand which region of the native reaction coordinate is mimicked by the $E{\cdot}AMP{\cdot}PP_i$ complex, nor have we identified the earliest point in the APS reaction to which

isomerization is linked. We are currently pursuing answers to these questions.

Conclusion. The catalytic cycle of the GTP subunit of ATP sulfurylase includes a substrate-induced isomerization that precedes and rate-limits the breaking of the β,γ-bond of GTP.

ACKNOWLEDGMENT

We thank Professor J. P. Richard, Department of Chemistry, University of Buffalo, for generously allowing us to perform the sequential-mixing, stopped-flow experiments in his laboratory.

REFERENCES

1. Bourne, H. R., Sanders, D. S., and McCormick, F. (1991) *Nature 349*, 117−126.
2. Sprang, S. R. (1997) *Annu. Rev. Biochem. 66*, 639−678.
3. Bourne, H. R., Sanders, D. A., and McCormick, F. (1990) *Nature 348*, 125−132.
4. Rodnina, M. V., Fricke, R., Kuhn, L., and Wintermeyer, W. (1995) *EMBO J. 14*, 2613−2619.
5. Moore, K. J. M., Webb, M. R., and Eccleston, J. F. (1993) *Biochemistry 32*, 7451−7459.
6. Rensland, H., Lautwein, A., Wittinghofer, A., and Goody, R. S. (1991) *Biochemistry 30*, 11181−11185.
7. Neal, S. E., Eccleston, J. F., and Webb, M. R. (1990) *Proc. Natl. Acad. Sci. U.S.A. 87*, 3562−3565.
8. Antonny, B., Chardin, P., Roux, M., and Chabre, M. (1991) *Biochemistry 30*, 8287−8295.
9. Eccleston, J. F., Moore, K. J. M., Brownbridge, G. G., Webb, M. R., and Lowe, P. N. (1991) *Biochem. Soc. Trans. 19*, 432−437.
10. Hiratsuka, T. (1983) *Biochim. Biophys. Acta 742*, 496−508.
11. Liu, C., Suo, Y., and Leyh, T. S. (1994) *Biochemistry 33*, 7309−7314.
12. Leyh, T. S., and Suo, Y. (1992) *J. Biol. Chem. 267*, 542−545.
13. Leyh, T. S., Taylor, J. T., and Markham, G. H. (1987) *J. Biol. Chem. 263*, 2409−2416.
14. Leyh, T. S., Vogt, T. F., and Suo, Y. (1992) *J. Biol. Chem. 267*, 10405−10410.
15. De Meio, R. M. (1975) in *Metabolic Pathways* (Greenberg, D. M., Ed.) Vol. VII, Academic Press, New York.
16. Singleton, R. J. (1993) in *The Sulfate Reducing Bacteria: Contemporary Perspectives* (Odom J. M., and Singleton, R. J., Eds.) pp 1−20, Springer-Verlag, New York.
17. Leyh, T. S. (1993) *Crit. Rev. Biochem. Mol. Biol. 28*, 515−542.
18. Zhang, H., Varlamova, O., Vargas, F. M., Falany, C. N., and Leyh, T. S. (1998) *J. Biol. Chem. 273*, 10888−10892.
19. Maniatis, T., Fritsch, E. F., and Sambrook, J. (1982) *Molecular Cloning: a Laboratory Manual*, Cold Spring Harbor Laboratory, Cold Spring Harbor, NY.
20. Yount, R. G. (1974) *Methods Enzymol. 38*, 420−427.
21. Tran-Dinh, S., and Roux, M. (1977) *Eur. J. Biochem. 76*, 245−249.
22. Yang, M., and Leyh, T. S. (1997) *Biochemistry 36*, 3270−3277.
23. John, J., Sohmen, R., Feuerstein, J., Linke, R., Wittinghofer, A., and Goody, R. S. (1990) *Biochemistry 29*, 6058−6065.
24. Ahmadian, M. R., Hoffman, U., Goody, R. S., and Wittinghofer, A. (1997) *Biochemistry 36*, 4535−4541.
25. Remmers, A. E., Posner, R., and Neubig, R. R. (1994) *J. Biol. Chem. 269*, 13771−13778.
26. Wagner, A., Simon, I., Sprinzl, M., and Goody, R. S. (1995) *Biochemistry 34*, 12535−12542.
27. Wang, R., Liu, C., and Leyh, T. S. (1995) *Biochemistry 34*, 490−495.
28. Johnson, K. A. (1992) *Enzymes (3rd Ed.) 20*, 1−61.
29. Johnson, K. A. (1986) *Methods Enzymol. 134*, 677−705.
30. Cleland, W. W. (1975) *Biochemistry 14*, 3220−3224.
31. Chant, J., and Stowers, L. (1995) *Cell 81*, 1−4.
32. Rodnina, M. V., Pape, T., Fricke, R., Kuhn, L., and Wintermeyer, W. (1996) *J. Biol. Chem. 271*, 646−652.
33. Remmers, A. E., and Neubig, R. R. (1996) *J. Biol. Chem. 271*, 4791−4797.
34. Wittinghofer, A., Scheffzek, K., and Ahmadian, R. (1997) *FEBS Lett. 410*, 63−67.
35. Moore, J. M., Lowe, P. N., and Eccleston, J. F. (1992) *Philos. Trans. R. Soc. London B 336*, 49−54.
36. Liu, C., Martin, E., and Leyh, T. S. (1994) *Biochemistry 33*, 2042−2047.
37. Leyh, T. S. (1998) *Methods Enzymol* (in press).
38. Jencks, W. P. (1980) *Adv. Enzymol. 51*, 75−106.

BI9817461